

Mass-Spectrometric Study of Ion-Molecule Reactions of CH_5^+, $C_2H_5^+$, and $C_3H_5^+$ with C_8–C_{18} Alcohols in an Ion Trap

Yuki Tanaka and Masaharu Tsuji[*,†]

Department of Applied Science for Electronics and Materials, Graduate School of Engineering Sciences, Kyushu University, Kasuga, Fukuoka 816-8580

†Institute of Advanced Material Study, Kyushu University, Kasuga, Fukuoka 816-8580

(Received February 20, 2002)

Chemical ionization of *n*-alkyl alcohols (*n*-C_xH_{2x+1}–OH = M; x=8–18) by the CH_5^+, $C_2H_5^+$, and $C_3H_5^+$ ions has been studied under a reactant-ion selective mode of an ion-trap type of GC/MS. In all reactions, $[M - H]^+$, alkyl $C_yH_{2y+1}^+$ (y = 3–x), and alkenyl $C_yH_{2y-1}^+$ (y = 4–x) ions were observed. On the basis of observed initial distributions and calculated thermochemical data, it was concluded that the major reactions for the formation of $C_yH_{2y+1}^+$ were proton transfer to a hydroxy group in the CH_5^+ reactions, proton transfer and/or hydroxide-ion abstraction in the $C_2H_5^+$ reactions, and $C_zH_{2z}OH^-$-ion ($z < x$) abstraction in the $C_3H_5^+$ reactions, while the major reactions for the formation of $C_yH_{2y-1}^+$ ions were proton transfer to alkyl chain in the CH_5^+ reactions, hydride-ion abstraction in the $C_2H_5^+$ reactions, and alkanide-ion abstraction in the $C_3H_5^+$ reactions.

The gas phase ion-molecule reactions of alcohol in a methane atmosphere have been studied by Munson and Field.[1] They measured CI mass spectra of *n*-$C_{10}H_{21}$–OH at a medium CH_4 pressure of 133 Pa, where dominant reactant ions were CH_5^+ (48%), $C_2H_5^+$ (40%), and $C_3H_5^+$ (6%). The $[M - H]^+$, $C_yH_{2y+1}^+$ ($y \leq x$), and $C_yH_{2y-1}^+$ ($y \leq x$) ions were observed as product ions. Here, x represents the number of carbons of alkyl group in a reagent, while y stands for the number of carbons of the alkyl group fragment. When methane was used as reactant in the CI technique, extensive fragmentation of alcohols occurred, and in particular, the intensity of ions in the molecular weight region (the $[M - H]^+$ ions) tended to be rather small.[2] Therefore, Field[2,3] used isobutene as reactant to diminish the amount of fragmentation occurring in the CI mass spectra of alcohols. He determined the isobutene CI mass spectra of 23 saturated, monohydroxylic alcohols. The main product ions were $[M - OH]^+ = R^+$ of ROH, $[M - H]^+$, $[M + H]^+$, $[M + C_4H_9 - H_2O]^+$, $[M + C_4H_9]^+$, and $[2M + H]^+$.

The medium-pressure CH_4 CI mass spectrometric study of *n*-$C_{10}H_{21}$–OH by Munson and Field[1] has been carried out without selecting reactant hydrocarbon ions. Therefore, the reactivity of dominant CH_5^+ and $C_2H_5^+$ reactant ions for *n*-$C_{10}H_{21}$–OH has not been determined. It is known that $C_3H_5^+$ ion is involved as a minor reactant ion when CH_4 is used as reactant.[1] However, no information has been obtained on its reactivity for alcohols. To the best of our knowledge, no CH_4 CI mass spectrometric study has been reported except for the pioneering work of Munson and Field[1] on *n*-$C_{10}H_{21}$–OH.

We have recently studied CH_4 CI mass spectra of *n*-paraffins (C_xH_{2x+2}; x = 8–18), 1-olefins (1-C_xH_{2x}; x = 8–18), and *n*-alkylbenzenes (PhC_xH_{2x+1}; x=3–13) by the CH_5^+, $C_2H_5^+$, and $C_3H_5^+$ ions using an ion-trap type of GC/MS.[4–6] In this study, CH_4 CI mass spectra of a series of alcohols (*n*-C_xH_{2x+1}–OH; x=8–18) by the CH_5^+, $C_2H_5^+$, and $C_3H_5^+$ ions are measured under a reactant-ion selective mode of an ion-trap type of GC/MS in order to study the effects of the hydroxyl group. The dependence of product-ion distributions on the reaction time was measured in order to determine initial product-ion distributions. The reactivity of CH_5^+, $C_2H_5^+$, and $C_3H_5^+$ for alcohols was discussed from the initial product-ion distributions and thermochemical calculations of heats of reactions.

Experimental

The CI mass spectrometer and the experimental conditions in this work were the same as those reported previously.[4–6] In brief, CI mass spectra were obtained using an ion-trap type of Hitachi M7200 GC/MS under a reactant-ion selective mode. One of the reactant CH_5^+, $C_2H_5^+$, and $C_3H_5^+$ ions produced from the subsequent fast ion-molecule reactions of CH_n^+ (n = 2–4) with CH_4 was selectively trapped as a reactant ion in an ion-trap cell. The maximum and average kinetic energies of the reactant ions in our apparatus were evaluated to be 10 and 4.2 eV (1 eV = 96.49 kJ mol^{-1}) for CH_5^+, 6.0 and 2.4 eV for $C_2H_5^+$, and 4.3 and 1.7 eV for $C_3H_5^+$, respectively, using a pseudo-potential well method.[5] These energies are higher than that in the medium-pressure CI experiments, which were estimated to be less than 1 eV.[7] The time for storing a reactant ion was kept constant at 5 ms. The ion-trap cell was kept at 170 °C. The reagents were diluted in hexane and injected into the GC with a high-purity carrier He gas. The partial pressures of CH_4 and He in an ion-trap cell were 9×10^{-3} and 7×10^{-3} Pa, respectively. The reaction time corresponding to the residence time in the ion-trap was varied from 0.5 to 40 ms. The mass spectra were measured at low reagent concentrations of about 1000–10000 pg cm^{-3} in order to reduce secondary ion-molecule reactions. It is known that the number of ions stored in the ion trap depends on the radio frequency voltage.[8] Thus, the CI mass spectra obtained in this study were calibrated against NIST

standard data.[9]

The operating conditions in the ion-trap cell used in this work were significantly different from those of the conventional medium-pressure CI mass spectrometer developed by Munson and Field.[1–3] In the medium-pressure CI measurements, the typical CH_4 gas pressure was 133 Pa and the residence time of reactant ions in the ionization-reaction chamber was about 10 μs. The total number of collisions of reactant ions with CH_4 during this residence time evaluated by Field[3] was about 200. In the present low-pressure CI measurements, the total number of collisions of a product ion with CH_4 and He was estimated to be about 1–100 times within the reaction time of 0.5–40 ms from a simple gas-kinetic hard-sphere collision model.

Results and Discussion

Contribution of Collisional Stabilization and Initial Product-Ion Distributions: When CI mass spectra resulting from ion-molecule reactions of CH_5^+, $C_2H_5^+$, and $C_3H_5^+$ with *n*-alcohols (*n*-C_xH_{2x+1}–OH; x = 8–18) were measured, $[M - H]^+$, $C_yH_{2y+1}^+$ (y = 3–x), and $C_yH_{2y-1}^+$ (y = 4–x) ions were observed. Although the $[M - H]^+ = C_xH_{2x}OH^+$ ions were observed, no $C_yH_{2y}OH^+$ ($y < x$) ions were observed. This indicates that the $C_yH_{2y}OH^+$ ions decompose completely into $C_yH_{2y-1}^+$ by loss of H_2O:

$$C_yH_{2y}OH^+ \rightarrow C_yH_{2y-1}^+ + H_2O. \quad (1)$$

The $\Delta H°$ values of reaction (1) are highly exothermic (approximately −2.1 eV).[9] Thus, the $C_yH_{2y}OH^+$ ions completely decompose into $C_yH_{2y-1}^+$. This result is contrasted with that for *n*-alkylbenzenes,[6] where the decomposition of $PhC_yH_{2y}^+$ into $C_yH_{2y-1}^+$ by loss of PhH was not observed:

$$PhC_yH_{2y}^+ \nrightarrow C_yH_{2y-1}^+ + PhH. \quad (2)$$

This can be explained by the lower exothermicity of reaction (2) ($\Delta H° \approx -1.3$ eV)[9] and the stabilization of $PhC_yH_{2y}^+$ by isomerization into tropylium-type ion.

If the collisional stabilization takes part in the formation of product ions, an excess energy will be partly relaxed by collisions with CH_4 and He gases. Therefore, fragmentation will be suppressed in CI mass spectra obtained at long reaction times (= residence time in the ion trap). In order to examine the contribution of collisional stabilization in our CI conditions, the dependence of product-ion distributions on the reaction time was measured. For example, Figs. 1 and 2 show product-ion distributions of $C_yH_{2y+1}^+$ (y = 3–x) and $C_yH_{2y-1}^+$ (y = 4–x) in the reactions of CH_5^+, $C_2H_5^+$, and $C_3H_5^+$ with typical reagents (*n*-C_xH_{2x+1}–OH; x = 8, 14, and 18) at five different reaction times; 0.5, 2, 10, 20, and 40 ms. The $C_yH_{2y+1}^+$ (y = 3–x) and $C_yH_{2y-1}^+$ (y = 4–x) distributions exhibit single peaks in most cases. It is clear from Figs. 1 and 2 that the $C_yH_{2y+1}^+$ and $C_yH_{2y-1}^+$ distributions depend on the reaction

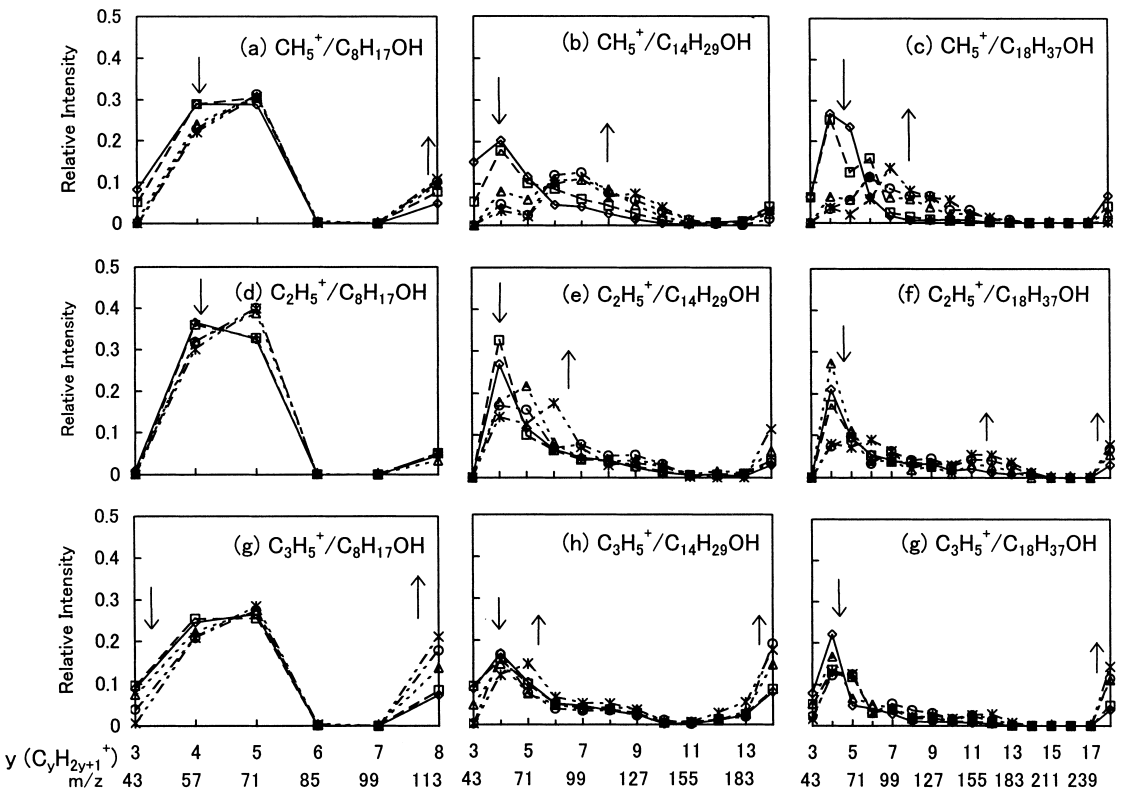

Fig. 1. Dependence of product-ion distributions of $C_yH_{2y+1}^+$ (y = 3–x) ion on the reaction time in the ion-molecule reactions of CH_5^+, $C_2H_5^+$, and $C_3H_5^+$ with $C_8H_{17}OH$, $C_{14}H_{27}OH$, and $C_{18}H_{37}OH$. Reaction time ◇: 0.5, □: 2, △: 10, ○: 20, and ×: 40 ms. Relative intensities were branching ratios of each ion for total product ions. Arrows indicate an increase or a decrease in product-ion distribution with an increasing the reaction time. The line connecting the points in the graphs is the $C_yH_{2y+1}^+$ formed from the same reaction time.

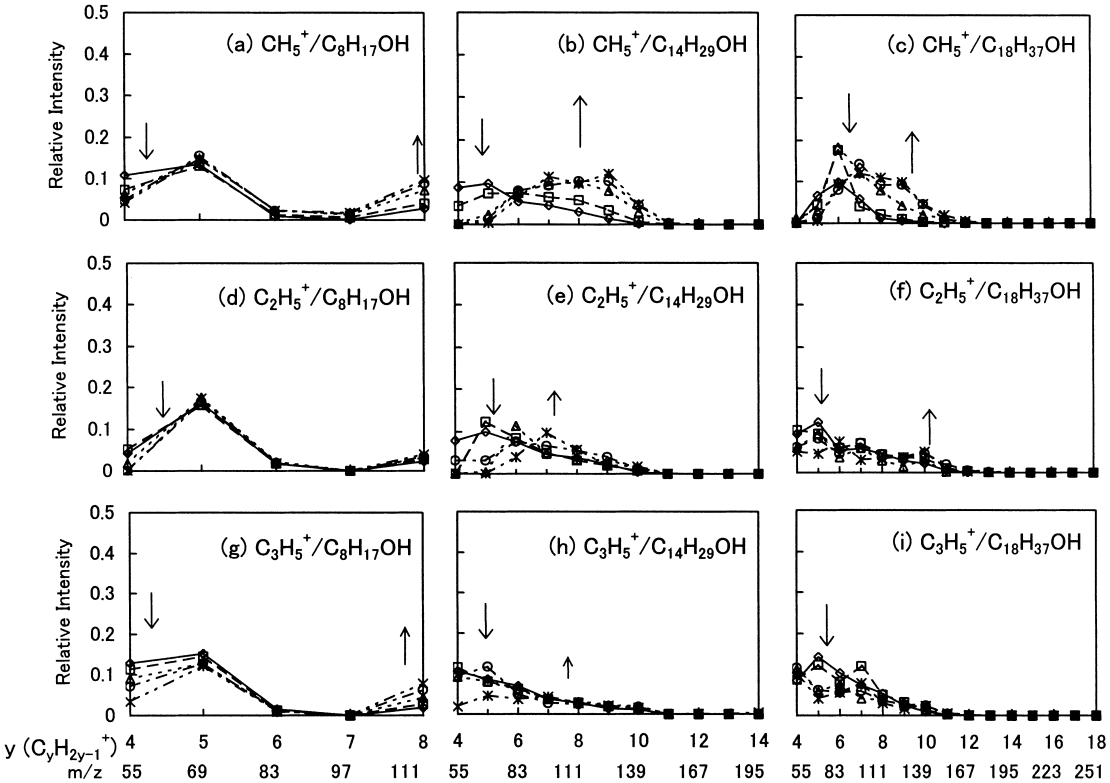

Fig. 2. Dependence of product-ion distributions of $C_yH_{2y-1}^+$ ($y = 4–x$) ion on the reaction time in the ion-molecule reactions of CH_5^+, $C_2H_5^+$, and $C_3H_5^+$ with $C_8H_{17}OH$, $C_{14}H_{27}OH$, and $C_{18}H_{37}OH$. Reaction time ◇:0.5, □:2, △:10, ○:20, and ×:40 ms. Relative intensities were branching ratios of each ion for total product ions. Arrows indicate an increase or a decrease in product-ion distribution with an increasing reaction time. The line connecting the points in the graphs is the $C_yH_{2y-1}^+$ formed from the same reaction time.

time in most cases. The decreases or increases in the production distributions with increasing the reaction time are shown by arrows in Figs. 1 and 2. In all the nine CH_5^+, $C_2H_5^+$, and $C_3H_5^+$ reactions shown in Fig. 1, the branching ratios of $C_yH_{2y+1}^+$ having small y values (y = 3–6) decrease, while those having large y values ($y = 7–x$) increase in many cases. On the other hand, the branching ratios of $C_yH_{2y-1}^+$ having small y values (y = 4–6) decrease, while those having large y values (y = 7–10) increase in many cases. These findings indicate that collisional stabilization with CH_4 and He participates in the formation of the product ions. Similar results were obtained for the other alcohols. Thus, the initial product distributions were determined by extrapolating the dependence of branching ratios of product ions on the reaction time to zero reaction time, as shown in Fig. 3 for the formation of $[M - H]^+$ from the reactions of $C_nH_5^+$ (n = 1–3) with n-C_8H_{17}–OH. The uncertainties of the initial branching-ratios were estimated to be within ±8%. Two major product ions are alkyl $C_yH_{2y+1}^+$ ($y \leq x$) and alkenyl $C_yH_{2y-1}^+$ ($y \leq x$) ions. Their initial distributions are determined and the formation mechanisms are discussed below.

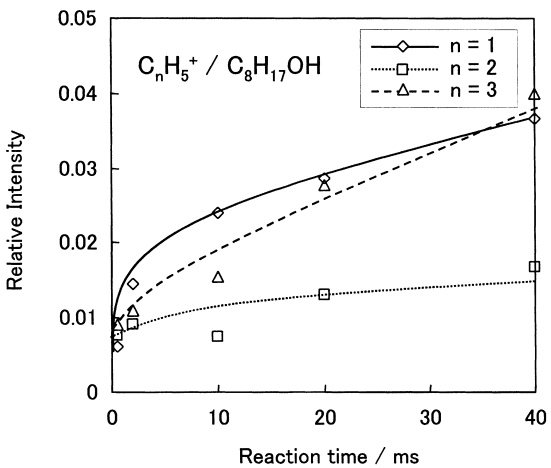

Fig. 3. Dependence of branching ratios of $[M - H]^+$ ions on the reaction time in the ion-molecule reactions of $C_nH_5^+$ (n = 1, 2, and 3) with $C_8H_{17}OH$. The lines are extrapolated to zero reaction time to find the initial product-ion distributions.

Distribution of Alkyl $C_yH_{2y+1}^+$ ($y = 3–x$) Ions: Figures 4(a)–4(i) show initial product-ion distributions of $C_yH_{2y+1}^+$ ($y = 3–x$) obtained for short (x = 8–10), medium (x = 11–14), and long (x = 15–18) chain reagents. The $C_yH_{2y+1}^+$ ($y = 3–x$) ions are observed in the CH_5^+, $C_2H_5^+$, and $C_3H_5^+$ reactions, and the intensity distributions are similar among the three reactions. In all reactions, the $C_yH_{2y+1}^+$ distributions peak at y = 4 for all (x = 8–18) chain reagents. In the $C_2H_5^+$ reactions, the $C_yH_{2y+1}^+$ distributions shift to higher y values than those in the CH_5^+ reactions. This implies that the excess energies released in the $C_2H_5^+$ reactions are smaller than those in the CH_5^+ reactions for the formation of $C_yH_{2y+1}^+$. The $C_yH_{2y+1}^+$ distribu-

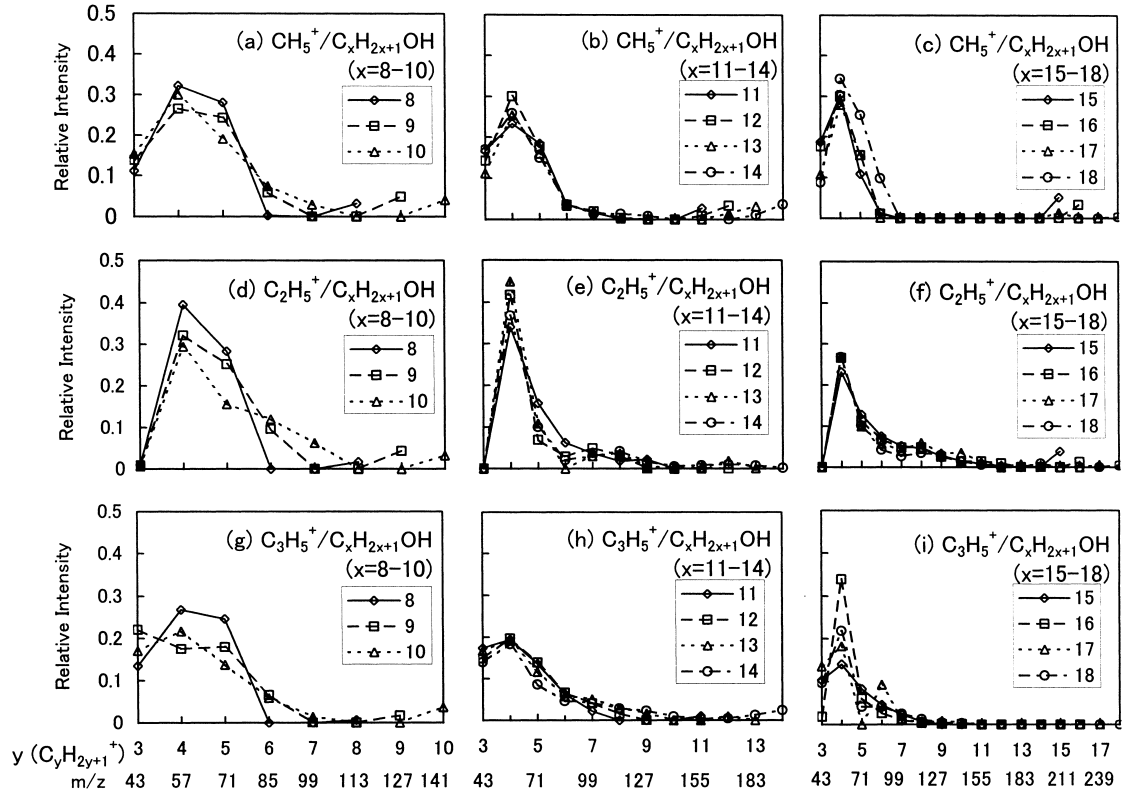

Fig. 4. Initial product-ion distributions of $C_yH_{2y+1}^+$ ($y = 3–x$) ion in the ion-molecule reactions of CH_5^+, $C_2H_5^+$, and $C_3H_5^+$ with C_8–C_{18} alcohols. (a),(d),(g) ◇: $C_8H_{17}OH$, □: $C_9H_{19}OH$, and △: $C_{10}H_{21}OH$; (b),(e),(h) ◇: $C_{11}H_{23}OH$, □: $C_{12}H_{25}OH$, △: $C_{13}H_{27}OH$, and ○: $C_{14}H_{29}OH$; (c),(f),(i) ◇: $C_{15}H_{31}OH$, □: $C_{16}H_{33}OH$, △: $C_{17}H_{35}OH$, and ○: $C_{18}H_{37}OH$. The largest $C_yH_{2y+1}^+$ ions correspond to the $C_xH_{2x+1}^+$ ions. The line connecting the points in the graphs is the alkyl $C_yH_{2y+1}^+$ ($y = 3–x$) ion formed from the same alcohol.

tions in the $C_3H_5^+$ reactions further shift to lower y values than those in the $C_2H_5^+$ reactions. This implies that larger excess energies are released in the $C_3H_5^+$ reactions than those in the $C_2H_5^+$ reactions for the formation of $C_yH_{2y+1}^+$.

Distribution of Alkenyl $C_yH_{2y-1}^+$ ($y = 4–x$) Ions: Figures 5(a)–5(i) show initial product-ion distributions of $C_yH_{2y-1}^+$ ($y = 4–x$) obtained for short ($x = 8–10$), medium ($x = 11–14$), long ($x = 15–18$) chain reagents. The $C_yH_{2y-1}^+$ ($y = 4–x$) ions are observed in the CH_5^+, $C_2H_5^+$, and $C_3H_5^+$ reactions. In all reactions, the $C_yH_{2y-1}^+$ distributions peak at $y = 4,5$ for all ($x = 8–18$) chain reagents. In the CH_5^+ reactions, the $C_yH_{2y-1}^+$ distributions are sharp, and the $C_yH_{2y-1}^+$ distributions in the $C_2H_5^+$ and $C_3H_5^+$ reactions are broader than those in the CH_5^+ reactions. The extent of fragmentation of $C_yH_{2y-1}^+$ in the $C_2H_5^+$ reactions is either similar to or lower than that in the CH_5^+ reactions. This implies that the excess energies released in the $C_2H_5^+$ reactions are similar to or smaller than those in the CH_5^+ reactions for the formation of $C_yH_{2y-1}^+$. The extent of fragmentation of $C_yH_{2y-1}^+$ in the $C_3H_5^+$ reactions is higher than that in the $C_2H_5^+$ reactions, indicating that the excess energies released in the $C_3H_5^+$ reactions are larger than those in the $C_2H_5^+$ reactions.

Alkyl and Alkenyl Total Ion Intensities: In Figs. 6(a)–6(c) we plot the sum of the intensities of all the $C_yH_{2y+1}^+$ ($y = 3–x$) ions and the sum of the intensities of all the $C_yH_{2y-1}^+$ ($y = 4–x$) ions formed from each of the straight-chain alcohols studied. In all reactions, total alkyl ions intensities decrease, while total alkenyl ions intensities increase with increasing x. As the size of alkyl group becomes larger, an increasing amount of attack at the alkyl chain occurs. On the other hand, such a significant change is not expected in the total amount of attack at the hydroxy group. The experimental results led us to conclude that alkyl ions are formed from the attack at the hydroxy group, while alkenyl ions are formed from the attack at the alkyl chain. These mechanisms are consistent with the predictions from reaction schemes, which will be shown later.

Comparison with the Previous CI Experiments: Field[1] measured CI mass spectra of alcohol (n-$C_{10}H_{21}$–OH) at a medium CH_4 pressure of 133 Pa. For example, his CI mass data of n-$C_{10}H_{21}$–OH are shown in Figs. 7(a) and 7(b), along with our corresponding data for the $C_nH_5^+$ (n=1–3) reactions, in order to examine the effects of collisional stabilization and kinetic energy of reactant ions. The extent of fragmentation in the $C_yH_{2y+1}^+$ and $C_yH_{2y-1}^+$distributions observed in this work is higher than that observed by Field et al.[1] One reason for the higher extent of fragmentation observed here may be lack of collisional stabilization under our experimental conditions. The other reason may be the difference in the kinetic energy of reactant ions. The maximum and average kinetic energies of reactant ions in our apparatus, given in the experimental section, are higher than those in the medium-pressure CI experiments, which were estimated to be less than 1 eV.[7]

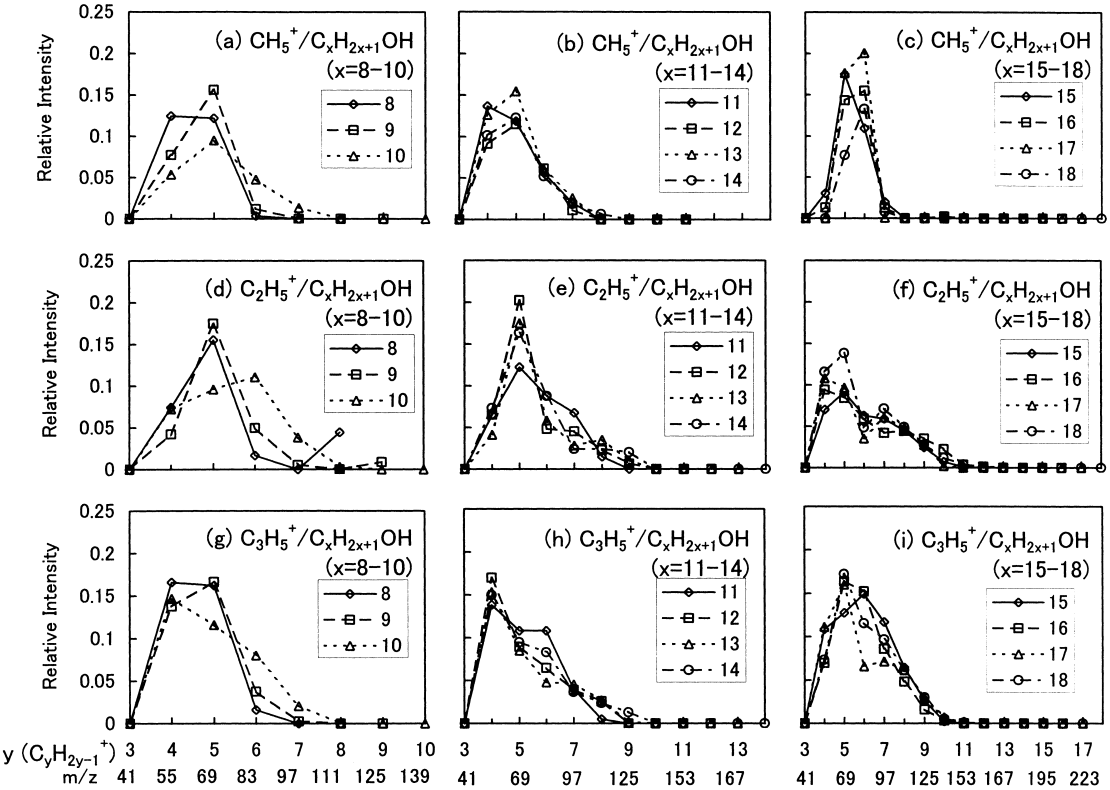

Fig. 5. Initial product-ion distributions of $C_yH_{2y-1}^+$ ($y = 4$–x) ion in the ion-molecule reactions of CH_5^+, $C_2H_5^+$, and $C_3H_5^+$ with C_8–C_{18} alcohols. (a),(d),(g) ◇: $C_8H_{17}OH$, □: $C_9H_{19}OH$, and △: $C_{10}H_{21}OH$; (b),(e),(h) ◇: $C_{11}H_{23}OH$, □: $C_{12}H_{25}OH$, △: $C_{13}H_{27}OH$, and ○: $C_{14}H_{29}OH$; (c),(f),(i) ◇: $C_{15}H_{31}OH$, □: $C_{16}H_{33}OH$, △: $C_{17}H_{35}OH$, and ○: $C_{18}H_{37}OH$. The largest $C_yH_{2y-1}^+$ ions correspond to the $C_xH_{2x-1}^+$ ions. The line connecting the points in the graphs is the alkenyl $C_yH_{2y-1}^+$ ($y = 4$–x) ion formed from the same alcohol.

Possible Mechanism and Energetics of Each Ion-Molecule Reaction: The possible formation processes of $C_yH_{2y+1}^+$ and $C_yH_{2y-1}^+$ by the XH^+ (X = CH_4, C_2H_4, and C_3H_4) reactions are shown in Scheme 1. The $C_yH_{2y+1}^+$ ions can be formed via proton transfer to a hydroxy group (A-1), hydroxide-ion abstraction (A-2), and $C_zH_{2z}OH^-$-ion abstraction (A-3). Here, z represents the carbon number of the alkyl group abstracted from a reagent. The $C_yH_{2y-1}^+$ ions can be formed via proton transfer to an alkyl group (B-1), hydride-ion abstraction (B-2), and alkanide-ion abstraction (B-3). In our previous study of the reactions of CH_5^+, $C_2H_5^+$, and $C_3H_5^+$ reactions with *n*-paraffins,[4] we found out that the formation channels of smaller $C_{y'}H_{2y'-1}^+$ ions ($y' < y$) through the fragmentation of $C_yH_{2y+1}^+$ are closed:

$$C_yH_{2y+1}^+ \nrightarrow C_{y'}H_{2y'-1}^+ + H_2, \quad (3a)$$

$$C_yH_{2y+1}^+ \nrightarrow C_{y'}H_{2y'-1}^+ + C_{y-y'}H_{2(y-y')+2}. \quad (3b)$$

The only fragmentation processes observed were:

$$C_yH_{2y+1}^+ \rightarrow C_{y'}H_{2y'+1}^+ + C_{y-y'}H_{2(y-y')}. \quad (4)$$

Thus, the formation of $C_{y'}H_{2y'-1}^+$ via $C_yH_{2y+1}^+$ ions is excluded from the list of possible reaction schemes.

The heats of reactions of each process for the formation of dominant $C_yH_{2y+1}^+$ and $C_yH_{2y-1}^+$ ions were calculated using reported thermochemical data.[9] The results obtained are shown in Figs. 8(A)–8(I) and 9(A)–9(I) for the cases of $x = 8$, 14, and 18 reagents. Similar energy relationships are obtained for the reactions of other *n*-alkyl alcohols. For example, $\Delta H°$ values in Fig. 8(A) represent the heats of reaction of the following reactions leading to various $C_yH_{2y+1}^+$ ($y \leq x$) ions from $x = 8$ reagent:

$$CH_5^+ + n\text{-}C_8H_{17}\text{–}OH \rightarrow C_xH_{2x+1}^+ + H_2O + CH_4,$$
$$\rightarrow C_yH_{2y+1}^+ + C_{8-y}H_{2(8-y)} + H_2O + CH_4.$$
(Reaction A-1 in Scheme 1) (5)

There are three possible $C_3H_5^+$ isomers, whose $\Delta H°$ values are 9.8, 10, and 11 eV for $CH_2{=}CHCH_2^+$, $CH_3C{=}CH_2^+$, and protonated cyclopropene ion, respectively.[9] Since the most stable $CH_2{=}CHCH_2^+$ isomer is a significant ion produced from CH_4 CI gas,[10] all thermochemical calculations for $C_3H_5^+$ are carried out using the above $\Delta H°$ value of $CH_2{=}CHCH_2^+$.

The $\Delta H°$ values in Figs. 8(A)–8(I) and 9(A)–9(I) are shown only for the formation of unstable $–CH_2^+$ (= $C_yH_{2y+1}^+$) and $–CH{=}CH^+$ (= $C_yH_{2y-1}^+$) ions, *n*-paraffins, and 1-olefins as ionic and neutral products for the sake of clarity. However, more stable isomers having secondary and tertiary alkyl groups may be formed. Since the $\Delta H°$ values of secondary

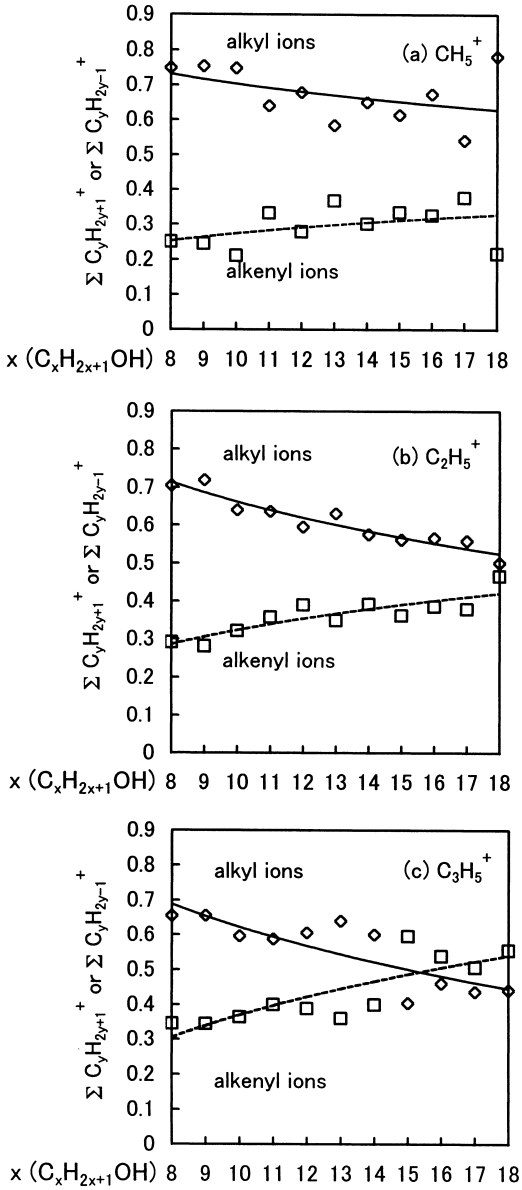

Fig. 6. Total alkyl and alkenyl ion intensities in the reactions of CH_5^+, $C_2H_5^+$, and $C_3H_5^+$ with C_8–C_{18} alcohols. (a) CH_5^+, (b) $C_2H_5^+$, and (c) $C_3H_5^+$. ◇: alkyl ion, □: alkenyl ion.

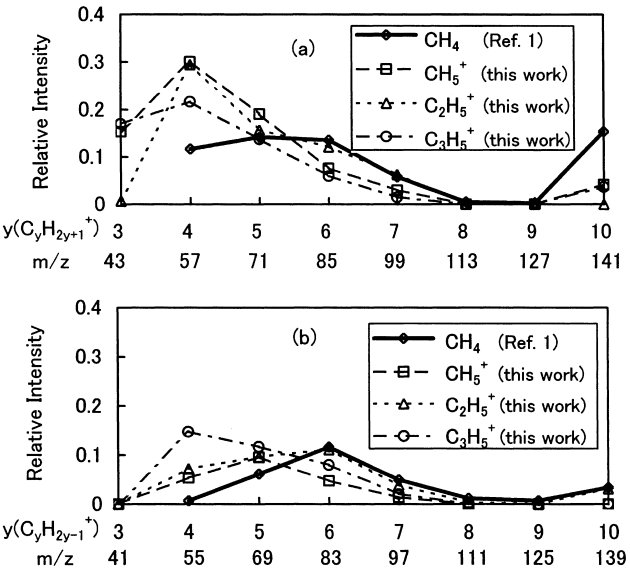

Fig. 7. CH_4 CI mass spectra of *n*-$C_{10}H_{21}$–OH obtained by Field et al. (Ref. 1) in a medium-pressure without selecting reactant ions and initial distributions in the CH_5^+, $C_2H_5^+$, and $C_3H_5^+$ reactions obtained in this study.

and tertiary carbocations are lower than those of primary ones by about 0.87 and 1.3 eV, respectively,[9] many endoergic processes change to exoergic ones for the formation of large $C_yH_{2y+1}^+$ and $C_yH_{2y-1}^+$ ions via stabilization due to isomerization. The $\Delta H°$ values for proton transfer channels (A-1) and (B-1) increase in the order of CH_5^+, $C_2H_5^+$, and $C_3H_5^+$ reactions due to increasing in the proton affinity in the order of CH_4 (PA = 5.7 eV), C_2H_4(7.1 eV) and C_3H_4 (8.0 eV).[9] On the other hand, there are no significant differences in the $\Delta H°$ values among the hydroxide-ion abstraction (A-2), $C_zH_{2z}OH^-$-ion abstraction (A-3), hydride-ion abstraction (B-2), and alkanide-ion abstraction (B-3). It is evident from Figs. 8(A)–8(I) and 9(A)–9(I) that the $\Delta H°$ values are essentially independent of chain length of fragment ions y for the formation of $C_yH_{2y+1}^+$, while they generally decrease with increasing y for the formation of $C_yH_{2y-1}^+$ without taking isomerization into account.

In the CH_5^+ reactions, reactions (A-1) and (B-1) are only possible for the formation of the $C_yH_{2y+1}^+$ and $C_yH_{2y-1}^+$ ions, respectively. It is clear from Figs. 8(A)–8(C) and Figs. 9(A)–9(C) that reactions (A-1) and (B-1) are exothermic without taking isomerization into account. Thus, the formation of $C_yH_{2y+1}^+$ and $C_yH_{2y-1}^+$ ions proceeds through proton-transfer to a hydroxy group (A-1) and through proton-transfer to alkyl portion (B-1), respectively.

In the $C_2H_5^+$ reactions, the $C_yH_{2y+1}^+$ ions can be formed via reactions (A-1), (A-2), and (A-3). It is clear from Figs. 8(D)–8(F) that $C_zH_{2z}OH^-$-ion abstraction (A-3) is more favorable than reactions (A-1) and (A-2) on the basis of energetics. A comparison of the $C_yH_{2y+1}^+$ distributions between $C_2H_5^+$ and CH_5^+ reactions indicated that the excess energies released in the $C_2H_5^+$ reactions are smaller than those in the CH_5^+ reactions. The $\Delta H°$ values of reactions (A-1) and (A-2) in the $C_2H_5^+$ reactions are higher than the $\Delta H°$ values of reactions (A-1) in the CH_5^+ reactions. There is only a small difference in $\Delta H°$ values (0.5 eV) between reactions (A-1) and (A-2). Therefore, it is reasonable to assume that $C_yH_{2y+1}^+$ ions are dominantly formed via proton transfer (A-1) and/or hydroxide-ion abstraction (A-2) in the $C_2H_5^+$ reactions.

In the $C_2H_5^+$ reactions, the $C_yH_{2y-1}^+$ ions can be formed via reactions (B-1), (B-2), and (B-3). It is clear from Figs. 9(D)–9(F) that hydride-ion abstraction (B-2) and alkanide-ion abstraction (B-3) are more favorable than reactions (B-1) on the basis of energetics. The $\Delta H°$ values for the formation of $C_yH_{2y-1}^+$ from reaction (B-2) in the $C_2H_5^+$ reactions are similar to or higher than those of (B-1) in the CH_5^+ reactions. A comparison of the extent of fragmentation of $C_yH_{2y-1}^+$ between the $C_2H_5^+$ and CH_5^+ reactions indicated that excess energies released in the $C_2H_5^+$ reactions are similar to or smaller than those in the CH_5^+ reactions. Consequently, it is reasonable to assume that $C_yH_{2y-1}^+$ ions are dominantly

(A) The formation of alkyl ion ($C_yH_{2y+1}^+$)

(A-1) Proton transfer by XH^+ (X = CH_4, C_2H_4, C_3H_4) by loss of H_2O and alkene

$$XH^+ + C_xH_{2x+1}OH \xrightarrow{-X} [M+H]^+ \; (= C_xH_{2x+1}OH_2^+) \xrightarrow{-H_2O} C_xH_{2x+1}^+ \longrightarrow C_yH_{2y+1}^+ + C_zH_{2z}$$

(A-2) Hydroxide ion (OH^-) abstraction by XH^+ (X = C_2H_4, C_3H_4) by loss of alkene

$$XH^+ + C_xH_{2x+1}OH \xrightarrow{-XHOH} C_xH_{2x+1}^+ \longrightarrow C_yH_{2y+1}^+ + C_zH_{2z}$$

(A-3) $C_zH_{2z}OH^-$ abstraction by XH^+ (X = C_2H_4, C_3H_4)

$$XH^+ + C_xH_{2x+1}OH \longrightarrow C_yH_{2y+1}^+ + C_zH_{2z}OH\text{–}XH$$

(B) The formation of alkenyl ion ($C_yH_{2y-1}^+$)

(B-1) Proton transfer by XH^+ (X = CH_4, C_2H_4, C_3H_4) by loss of H_2, H_2O, and alkene

$$XH^+ + C_xH_{2x+1}OH \xrightarrow{-X} [M+H]^+ \; (= C_xH_{2x+2}OH^+) \xrightarrow{-H_2} C_xH_{2x-1}OH_2^+ \xrightarrow{-H_2O} C_yH_{2y-1}^+ + C_zH_{2z}$$

(B-2) Hydride ion (H^-) abstraction by XH^+ (X = C_2H_4, C_3H_4)

$$XH^+ + C_xH_{2x+1}OH \xrightarrow{-XH_2} C_xH_{2x-1}OH_2^+ \xrightarrow{-H_2O} C_yH_{2y-1}^+ + C_zH_{2z}$$

(B-3) Alkanide ion ($C_zH_{2z+1}^-$) abstraction by XH^+ (X = C_2H_4, C_3H_4)

$$XH^+ + C_xH_{2x+1}OH \xrightarrow{-XH\,C_zH_{2z+1}} C_yH_{2y-1}OH_2^+ \xrightarrow{-H_2O} C_yH_{2y-1}^+$$

Scheme 1. Reaction scheme of the ion-molecule reactions of XH^+ (X = CH_4, C_2H_4, and C_3H_4) with alcohols.

formed via hydride-ion abstraction (B-2) in the $C_2H_5^+$ reactions.

In the $C_3H_5^+$ reactions, the reactions (A-1), (A-2), and (A-3) are possible for the formation of $C_yH_{2y+1}^+$ ions. It is clear from Figs. 8(G)–8(I) that $C_zH_{2z}OH^-$-ion abstraction (A-3) is more favorable than reactions (A-1) and (A-2) on the basis of thermochemical data. The extent of fragmentation of $C_yH_{2y+1}^+$ indicated that the excess energies released in the $C_3H_5^+$ reactions are similar to or higher than the excess energies released in the $C_2H_5^+$ reactions. The $\Delta H°$ values for the formation of $C_yH_{2y+1}^+$ from reactions (A-3) in the $C_3H_5^+$ reactions are smaller than those of (A-2) in the $C_2H_5^+$ reactions, and there are no more low-energy reaction pathways leading to $C_yH_{2y+1}^+$ in the $C_3H_5^+$ reactions. It is therefore reasonable to assume that $C_yH_{2y+1}^+$ ions are dominantly formed via lowest energy $C_zH_{2z}OH^-$-ion abstraction (A-3) in the $C_3H_5^+$ reactions. The higher extent of fragmentation in the $C_3H_5^+$ reactions than in the $C_2H_5^+$ reactions is attributed to higher extent

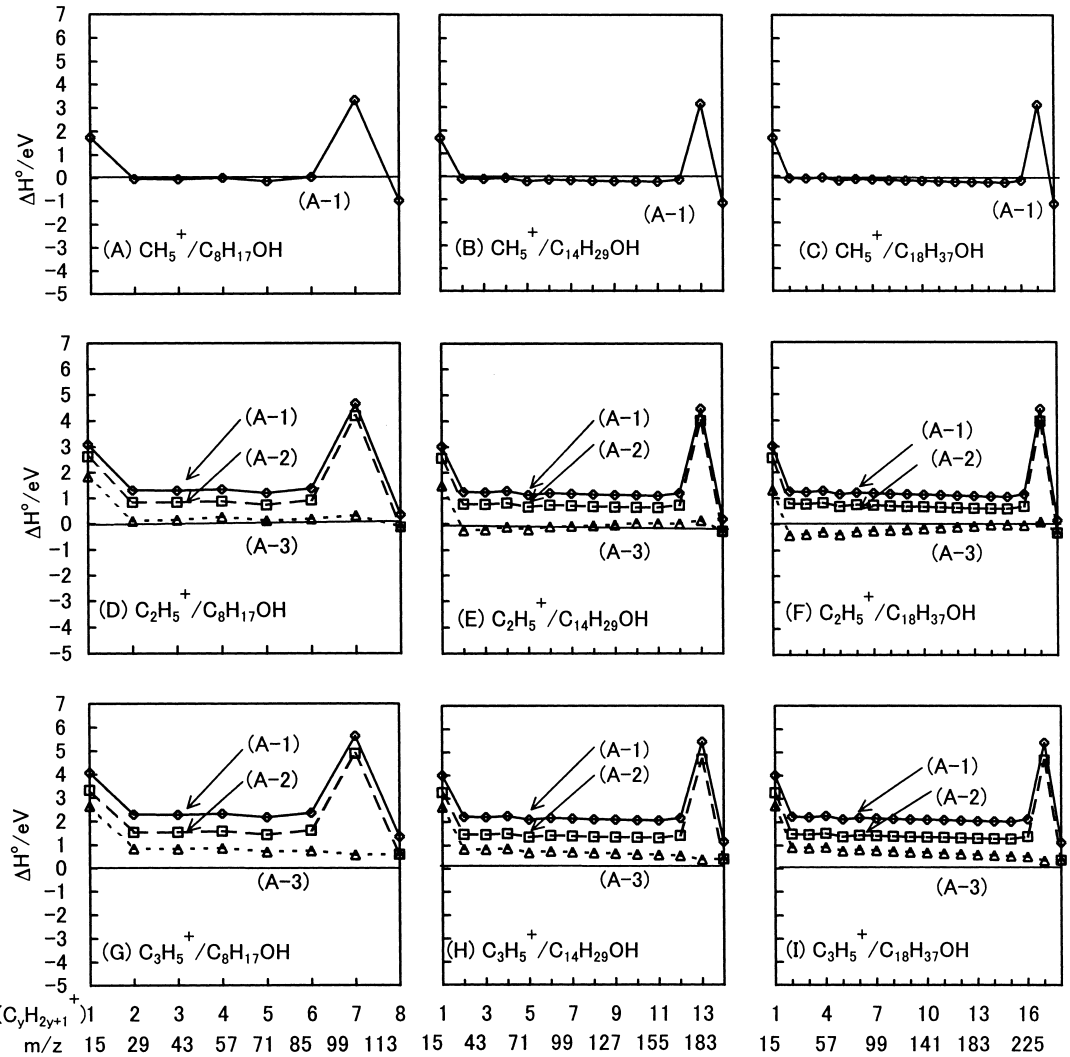

Fig. 8. Energy relations in the ion-molecule reactions of CH_5^+, $C_2H_5^+$, and $C_3H_5^+$ with *n*-C_8H_{17}–OH, *n*-$C_{14}H_{27}$–OH, and *n*-$C_{18}H_{37}$–OH leading to *n*-$C_yH_{2y+1}^+$. ◇: (A-1) Proton transfer, □: (A-2) hydroxide-ion abstraction, △: (A-3) $C_zH_{2z}OH^-$-ion abstraction. The largest $C_yH_{2y+1}^+$ ions correspond to the $C_xH_{2x+1}^+$ ions. The line connecting the points in the graphs is the $C_yH_{2y+1}^+$ formed from the same reaction pathway. $\Delta H°$ values are shown in eV units (1 eV = 96.485 kJ mol^{-1}).

of isomerization in the former reactions.

In the $C_3H_5^+$ reactions, the reactions (B-1), (B-2), and (B-3) are possible for the formation of $C_yH_{2y-1}^+$ ions. It is clear from Figs. 9(G)–9(I) that alkanide-ion abstraction (B-3) is more favorable than reactions (B-1) and (B-2) on the basis of energetics. The $\Delta H°$ values for the formation of $C_yH_{2y-1}^+$ from reaction (B-3) in the $C_3H_5^+$ reactions are similar to or smaller than those of (B-2) in the $C_2H_5^+$ reactions. The extent of fragmentation of $C_yH_{2y-1}^+$ implied that the excess energies released in the $C_3H_5^+$ reactions are larger than those in the $C_2H_5^+$ reactions. Consequently, it is reasonable to assume that $C_yH_{2y-1}^+$ ions are dominantly formed via lowest energy alkanide-ion abstraction (B-3) in the $C_3H_5^+$ reactions.

Concluding Remarks: The gas-phase ion-molecule reactions of CH_5^+, $C_2H_5^+$, and $C_3H_5^+$ with alcohols (*n*-C_xH_{2x+1}–OH; x=8–18) have been studied in an ion-trap type of GC/MS by separating each reactant ion. In all reactions, $C_yH_{2y+1}^+$ (y = 3–x), $C_yH_{2y-1}^+$ (y = 4–x), and $[M - H]^+$ ions were observed. The lack of $C_yH_{2y}OH^+$ ions indicated their complete decomposition into $C_yH_{2y-1}^+$ by loss of H_2O. The dependence of the relative intensities of product ions on the reaction times indicated that collisional stabilization took part in the formation of some product ions. On the basis of the product-ion distributions and the energetics, major reaction mechanisms for the formation of $C_yH_{2y+1}^+$ and $C_yH_{2y-1}^+$ ions were discussed. The dominant formation processes of $C_yH_{2y+1}^+$ ions are proton transfer to a hydroxyl group in the CH_5^+ reactions, and proton transfer and/or hydroxide-ion abstraction in the $C_2H_5^+$, and $C_zH_{2z}OH^-$-ion abstraction in the $C_3H_5^+$ reactions. On the other hand, the dominant formation processes of $C_yH_{2y-1}^+$ ions are proton transfer to alkyl chain in the CH_5^+ reactions, and hydride-ion abstraction in the $C_2H_5^+$ reactions, and alkanide-ion abstraction in the $C_3H_5^+$ reactions. Further detailed experimental and theoretical studies are required to confirm the above prediction.

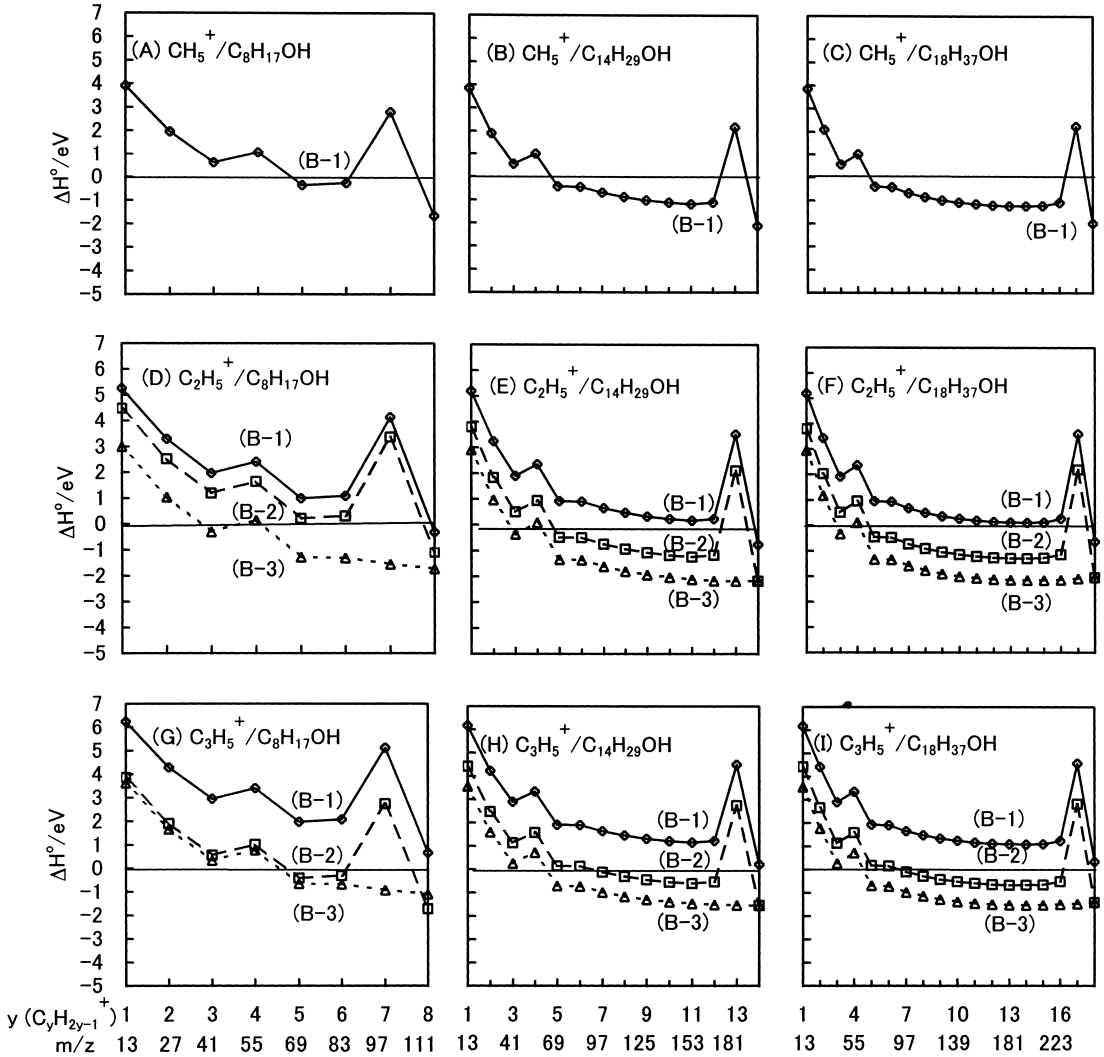

Fig. 9. Energy relations in the ion-molecule reactions of CH_5^+, $C_2H_5^+$, and $C_3H_5^+$ with *n*-C_8H_{17}–OH, *n*-$C_{14}H_{27}$–OH, and *n*-$C_{18}H_{37}$–OH leading to $C_yH_{2y-1}^+$. ◇: (B-1) Proton transfer, □: (B-2) hydride-ion abstraction, △: (B-3) alkanide-ion abstraction. The largest $C_yH_{2y-1}^+$ ions correspond to the $C_xH_{2x-1}^+$ ions. The line connecting the points in the graphs is the $C_yH_{2y-1}^+$ formed from the same reaction pathway. $\Delta H°$ values are shown in eV units (1 eV = 96.49 kJ mol^{-1}).

The authors acknowledge financial support from a Grant-in-Aid for Scientific Research No. 13558056 from the Ministry of Education, Science, Sports and Culture, and from Kyushu University Interdisciplinary Programs in Education and Projects in Research Development (2001–2002).

References

1 M. S. B. Munson and F. H. Field, *J. Am. Chem. Soc.*, **88**, 2621 (1966).

2 F. H. Field, *J. Am. Chem. Soc.*, **92**, 2672 (1970).

3 F. H. Field, in "Mass Spectrometry," MTP Intern. Rev. Soc., Phys. Chem. Ser. 1, ed by A. Maccoll, Butterworths, London (1972), Vol. 5, pp. 133–181.

4 Y. Tanaka, M. Tsuji, and Y. Nishimura, *Bull. Chem. Soc. Jpn.*, **73**, 2703 (2000).

5 Y. Tanaka and M. Tsuji, *Bull. Chem. Soc. Jpn.*, **74**, 839 (2001).

6 Y. Tanaka and M. Tsuji, *Bull. Chem. Soc. Jpn.*, **75**, 241 (2002).

7 C. Chang, G. G. Meisels, and J. A. Taylor, *Int. J. Mass Spectrom. Ion Phys.*, **12**, 411 (1973).

8 Y. Malinovich, R. Arakawa, G. Haase, and C. Lifshitz, *J. Phys. Chem.*, **89** 2253 (1985).

9 S. G. Lias, J. E. Bartmess, J. F. Liebman, J. L. Holmes, R. D. Levin, and W. G. Mallard, *J. Phys. Chem. Ref. Data*, **17**, Suppl. 1 (1988); Updated data were obtained from NIST Standard Ref. Database, Number 69, 2001, (http://webbook.nist.gov/chemistry).

10 R. Houriet, T. A. Elwood, and J. H. Futrell, *J. Am. Chem. Soc.*, **100**, 2320 (1978).